Naturwissenschaften (2004) 91:157–172
DOI 10.1007/s00114-004-0516-x

REVIEW

Andreas Züttel

Hydrogen storage methods

Published online: 17 March 2004

Abstract Hydrogen exhibits the highest heating value per mass of all chemical fuels. Furthermore, hydrogen is regenerative and environmentally friendly. There are two reasons why hydrogen is not the major fuel of today's energy consumption. First of all, hydrogen is just an energy carrier. And, although it is the most abundant element in the universe, it has to be produced, since on earth it only occurs in the form of water and hydrocarbons. This implies that we have to pay for the energy, which results in a difficult economic dilemma because ever since the industrial revolution we have become used to consuming energy for free. The second difficulty with hydrogen as an energy carrier is its low critical temperature of 33 K (i.e. hydrogen is a gas at ambient temperature). For mobile and in many cases also for stationary applications the volumetric and gravimetric density of hydrogen in a storage material is crucial. Hydrogen can be stored using six different methods and phenomena: (1) high-pressure gas cylinders (up to 800 bar), (2) liquid hydrogen in cryogenic tanks (at 21 K), (3) adsorbed hydrogen on materials with a large specific surface area (at T<100 K), (4) absorbed on interstitial sites in a host metal (at ambient pressure and temperature), (5) chemically bonded in covalent and ionic compounds (at ambient pressure), or (6) through oxidation of reactive metals, e.g. Li, Na, Mg, Al, Zn with water. The most common storage systems are high-pressure gas cylinders with a maximum pressure of 20 MPa (200 bar). New lightweight composite cylinders have been developed which are able to withstand pressures up to 80 MPa (800 bar) and therefore the hydrogen gas can reach a volumetric density of 36 kg·m^{-3}, approximately half as much as in its liquid state. Liquid hydrogen is stored in cryogenic tanks at 21.2 K and ambient pressure. Due to the low critical temperature of hydrogen (33 K), liquid hydrogen can only be stored in open systems. The volumetric density of liquid hydrogen is 70.8 kg·m^{-3}, and large volumes, where the thermal losses are small, can cause hydrogen to reach a system mass ratio close to one. The highest volumetric densities of hydrogen are found in metal hydrides. Many metals and alloys are capable of reversibly absorbing large amounts of hydrogen. Charging can be done using molecular hydrogen gas or hydrogen atoms from an electrolyte. The group one, two and three light metals (e.g. Li, Mg, B, Al) can combine with hydrogen to form a large variety of metal–hydrogen complexes. These are especially interesting because of their light weight and because of the number of hydrogen atoms per metal atom, which is two in many cases. Hydrogen can also be stored indirectly in reactive metals such as Li, Na, Al or Zn. These metals easily react with water to the corresponding hydroxide and liberate the hydrogen from the water. Since water is the product of the combustion of hydrogen with either oxygen or air, it can be recycled in a closed loop and react with the metal. Finally, the metal hydroxides can be thermally reduced to metals in a solar furnace. This paper reviews the various storage methods for hydrogen and highlights their potential for improvement and their physical limitations.

A. Züttel (✉)
Physics Department,
University of Fribourg,
Pérolles, 1700 Fribourg, Switzerland
e-mail: Andreas.Zuettel@unifr.ch
Tel.: +41-26-3009086
Fax: +41-26-3009747

Introduction

Human beings developed on an earth based on plants, i.e. biomass, as the only energy carrier. The average power consumed by a human body at rest is 0.1 kW and approximately 0.4 kW for a hard-working body, delivering about 0.1 kW of work. The consumption of plants did not change the environment because the carbon dioxide liberated by humans and animals was reabsorbed by plants during photosynthesis. In 1792 Thomas Newcomen discovered the steam engine (Wilson 1981). For the first time, a nonliving machine worked for human beings and the foundation for an industrialized society was laid down. The energy for the steam engine was found in the

form of mineral coal; solar energy stored in the earth's crust over millions of years. Furthermore, the energy was obtained for free, one only had to pay for the mining. Coal as a solid energy carrier was later complemented by liquid crude oil and natural gas. Not only did the state of the energy carrier change with time, but also the amount of hydrogen in the fuel increased. World energy consumption increased from 5×10^{12} kWh/year in 1860 to 1.2×10^{14} kWh/year today. More than 1.0×10^{14} kWh/year (80%) is based on fossil fuels (coal, oil and gas). The population of human beings has increased in the last century by a factor of 6 but energy consumption has risen by a factor of 80 (Jochem 1991). The world-wide average continuous power consumption today is 2 kW/person. In the USA, the power consumption is on average 10 kW/person and in Europe about 5 kW/person, although there are two billion people on earth who do not consume any fossil fuels et all. The reserves of fossil fuels on earth are limited and predictions based on the continuation of the energy consumption development show that demand will soon exceed supply. Furthermore, the consumption of fossil fuels is responsible for the increase in the carbon dioxide in the atmosphere of approximately 3×10^{12} kg C/year (Watson 2001). Carbon dioxide is a greenhouse gas and causes an increase in the average temperature on earth. The major problem is the fact, that a large amount (approximately 98%) of the carbon dioxide on earth is dissolved in the water of the oceans (7.5×10^{14} kg C in the atmosphere, 4.1×10^{16} kg C in the oceans). About 2×10^{12} kg C per year dissolves in the water of the ocean. The solubility of carbon dioxide decreases with the increasing temperature of water by approximately 3%/K. If the average temperature of the oceans increases, the carbon dioxide solubility equilibrium between atmosphere and ocean shifts towards the atmosphere and leads to an reduction in the CO_2 flux into the ocean and therefore to an additional increase of the greenhouse gas in the atmosphere.

Considering the historical development of the energy carriers towards more hydrogen-rich fuels and the necessity to reduce carbon dioxide emissions, then hydrogen should be the energy carrier of the future:

$$\mathrm{C\ (coal)} \rightarrow -\mathrm{CH_2}- \mathrm{(oil)} \rightarrow \mathrm{CH_4(natural\ gas)} \rightarrow \mathrm{H_2(hydrogen)}$$

The series also shows a development going from a solid to a liquid and then finally to a gas-state energy carrier. Hydrogen is the most abundant element on earth; however, less than 1% is present as molecular hydrogen gas H_2, the overwhelming majority is chemically bound as H_2O in water and some is bound to liquid or gaseous hydrocarbons (Schlapbach and Züttel 2001). The production of hydrogen by means of electrolysis consumes electricity, which is physical work. Due to the limitations of the Carnot cycle, only approximately one-third of heat can be converted into work. This is the reason why energy stored in hydrogen is about three times more expensive than oil (IEA 2002). Chemical energy is based on the energy of unpaired outer electrons (valence electrons) which are to be stabilized by electrons from other atoms. The hydrogen atom is most attractive because its electron (for charge neutrality) is accompanied by only one proton, i.e. hydrogen has the highest ratio number of valence electrons to protons (and neutrons) of all the elements in the periodic table. The energy gain per electron is very high. The chemical energy per mass of hydrogen (39.4 $\mathrm{kWh\cdot kg^{-1}}$) is three times larger than that of other chemical fuels, e.g. liquid hydrocarbons (13.1 $\mathrm{kWh\cdot kg^{-1}}$) (Weast 1976). In other words, the energy content of 0.33 kg of hydrogen corresponds to the energy content of 1 kg of oil. The energy content of a fuel is usually called the heating value. The difference between the upper and the lower heating value is the enthalpy of vaporization of water according to the state of the water as a result of combustion. For hydrogen the lower heating value is 33.3 $\mathrm{kWh\cdot kg^{-1}}$, and the upper heating value is 39.4 $\mathrm{kWh\cdot kg^{-1}}$. Hydrogen is the most abundant of all elements in the universe, and it is thought that the heavier elements were, and still are, being built from hydrogen and helium. It has been estimated that hydrogen makes up more than 90% of all the atoms or 75% of the mass of the universe (Weast 1976).

There is a technical and an economic challenge to overcome before the hydrogen energy economy becomes reality. The technical challenge is the real-time production, the safe and convenient storage and the efficient combustion of hydrogen. In order to satisfy the world's demand for fossil fuels, more than 3×10^{12} kg hydrogen would have to be produced per year. This is roughly 100 times the present hydrogen production. The solar constant is 1.369 $\mathrm{kW\cdot m^{-2}}$ and approximately 50% of the solar radiation reaches the surface of the earth. Photovoltaic systems have an efficiency of approximately 10%, which is the same for biological systems based on photosynthesis; corn (maize) is one of the plants with a photoconversion efficiency of about 10%. In the best-case scenario, half of the time is night and, therefore, under ideal conditions about 541,000 $\mathrm{km^2}$ (90 $\mathrm{m^2}$/person) covered with photovoltaic cells would be necessary to produce the present-day world energy consumption. This is a square with sides each measuring 740 km.

The economic challenge is the cost of hydrogen production. The world economy today is based on free energy naturally stored over millions of years. The price we are used to paying for fossil fuels is the mining cost only. In order to adapt the world to a synthetic fuel such as hydrogen, the world economy needs to be convinced of the benefits in order to see the need to pay for the energy content of the fuel too. Renewable energy requires in general an investment of approximately 5 years for the energy production. This means an investment of approximately €10^{13}–10^{14} (€1≈US$1) or in words 10–100 trillion euros, i.e. the same amount as is spent worldwide for energy within 5 years. The investment corresponds to approximately 20% of the annual income of a person who lives in a highly industrialized country.

Today's worldwide consumption of hydrogen as a chemical raw material (about 5×10^{10} kg/year) is produced to a large extent using fossil fuels by means of the reaction $-CH_2- + 2H_2O \rightarrow 3H_2 + CO_2$ at an elevated temperature (>850°C). This reaction is endothermic and therefore consumes energy, 8.9 kWh·kg^{-1} hydrogen. However, the hydrogen production from fossil fuels is not renewable and produces at least the same amount of carbon dioxide as the direct combustion of the fossil fuel.

Hydrogen is a renewable fuel, but only if the hydrogen is produced directly from solar light or indirectly via electricity from a renewable source e.g. wind-power or hydro-power. Some of the earliest work in solar thermochemistry was dedicated to the direct thermal dissociation of water, also known as thermolysis of water, i.e. $H_2O \rightarrow H_2 + 1/2\ O_2$. The processes investigated to date used a zirconia surface, solar-heated to temperatures of or above 2,500 K, and subjected to a stream of water vapour (Steinfeld and Palumbo 2001). The gaseous products that result from the thermolysis of water need to be separated at high temperatures to avoid recombination or ending up with an explosive mixture. Among the ideas proposed for separating the H_2 from the products are effusion separation, and electrolytic separation. Rapid quenching by injecting a cold gas or by expansion in a nozzle, followed by a low-temperature separation, are simpler and workable, but the quenching introduces a significant drop in the exergy efficiency of the process. Furthermore, the very high temperatures demanded by the thermodynamics of the process pose severe material problems and can lead to significant re-radiation from the reactor, thereby lowering the absorption efficiency and, consequently, further lowering the energy efficiency. These obstacles pushed the research in the direction of water-splitting thermochemical cycles.

Electricity from a renewable energy source, e.g. wind power, photovoltaics, hydropower and geothermal power, can be used for the electrolysis of water. Electrolysis at ambient temperature and ambient pressure requires a minimum voltage of 1.481 V and therefore a minimum energy of 39.7 kWh·kg^{-1} hydrogen. These days, electrolyser systems consume approximately 47 kWh·kg^{-1} hydrogen; i.e. the efficiency is approximately 85% (GTec 2002).

Hydrogen can be transported in pipelines in a similar way to natural gas. There are networks for hydrogen already in operation; a 1,500-km network in Europe and a 720-km network in the USA. The oldest hydrogen pipe network is in the Ruhr area in Germany and has operated for more than 50 years. The tubes with a typical diameter of 25–30 cm are built using conventional pipe steel and operate at a pressure of 10–20 bar. The volumetric energy density of hydrogen gas is 36% of the volumetric energy density of natural gas at the same pressure. In order to transport the same amount of energy, the hydrogen flux has to be 2.8 times larger than the flux of natural gas. However, the viscosity of hydrogen (8.92×10^{-6} Pa s) is significantly smaller than that of natural gas (11.2×10^{-6} Pa s). The minimum power P required to pump a gas through a pipe is given by

$$P = 8\pi l v^2 \eta \quad (1)$$

where l is the length of the pipe, v the velocity and η the dynamic viscosity of the gas. The transmission power per energy unit is therefore 2.2 times larger for hydrogen than for natural gas. The total energy loss during the transportation of hydrogen is about 4% of the energy content. Because of its great length, and therefore the great volume of piping systems, a slight change in the operating pressure of a pipeline system results in a large change of the amount of hydrogen gas contained within the piping network. Therefore, the pipeline can be used to handle fluctuations in supply and demand, avoiding the cost of onsite storage.

Hydrogen storage

The ordinary isotope of hydrogen, H, is known as protium (Weast 1976) and has an atomic weight of 1 (1 proton and 1 electron). In 1932, the isolation of a stable isotope was announced (Urey et al. 1932), deuterium (D) with an atomic weight of 2 (1 proton and 1 neutron, 1 electron). Two years later an unstable isotope, tritium (T), with an atomic weight of 3 (1 proton and 2 neutron, 1 electron) was discovered. Tritium has a half-life of about 12.5 years (Weast 1976). One atom of deuterium is found in about 6,000 ordinary hydrogen atoms (0.017%). Tritium atoms are also present 10^{-18}% (Shleien et al. 1998) as a result of natural processes in the atmosphere, as well as from fallout from past atmospheric nuclear weapons tests and the operation of nuclear reactors and fuel reprocessing plants. All the isotopes of hydrogen react together and form, due to the single electron in the atom, covalent molecules like H_2, D_2 and T_2, respectively. Hydrogen has a very ambivalent behaviour to other elements, it occurs as anion (H^-) or cation (H^+) in ionic compounds; it participates with its electron to form covalent bonds e.g. with carbon; and it can even behave like a metal and form alloys at ambient temperature.

The hydrogen molecule H_2 can be found in various forms depending on the temperature and the pressure, which are shown in the phase diagram (Fig. 1). At low temperatures hydrogen is a solid with a density of 70.6 kg·m^{-3} at −262°C and is a gas at higher temperatures with a density of 0.089886 kg·m^{-3} at 0°C and a pressure of 1 bar. A small zone starting at the triple point and ending at the critical point exhibits the liquid hydrogen with a density of 70.8 kg·m^{-3} at −253°C. At ambient temperature (298.15 K) hydrogen is a gas and can be described by the Van der Waals equation:

$$p(V) = \frac{nRT}{V - nb} - a \cdot \frac{n^2}{V^2} \quad (2)$$

where p is the gas pressure, V the volume, T the absolute temperature, n the number of moles, R the gas constant

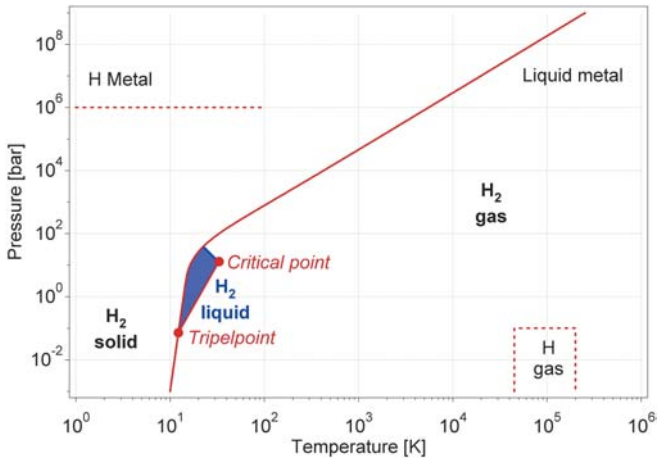

Fig. 1 Primitive phase diagram for hydrogen. Liquid hydrogen only exists between the *solid line* and the line from the triple point at 21.2 K and the critical point at 32 K

(R=8.314 J·K^{-1}·mol^{-1}), a is the dipole interaction or repulsion constant (a=2.476×10^{-2} m^6·Pa·mol^{-2}) and b is the volume occupied by the hydrogen molecules (b=2.661×10^{-5} m^3·mol^{-1}) (Weast 1976). The strong repulsion interaction between hydrogen molecules is responsible for the low critical temperature (T_c=33 K) of hydrogen gas. Hydrogen storage basically implies the reduction of the enormous volume of the hydrogen gas; 1 kg of hydrogen at ambient temperature and atmospheric pressure takes a volume of 11 m^3. In order to increase the hydrogen density in a storage system, work must either be applied to compress hydrogen, or the temperature has to be decreased below the critical temperature, or finally, the repulsion has to be reduced by the interaction of hydrogen with another material. The second important criterion for a hydrogen storage system is the reversibility of the hydrogen uptake and release. This criterion excludes all covalent hydrogen carbon compounds as hydrogen storage materials, because the hydrogen is only released from carbon hydrogen compounds if they are heated to temperatures above 800°C or if the carbon is oxidized. There are basically six possible methods that can be used in order to reversibly store hydrogen with a high volumetric and gravimetric density (see Table 1). The following sections focus on these methods and illustrate their advantages and disadvantages.

High-pressure gas cylinders

The most common storage system are high-pressure gas cylinders with a maximum pressure of 20 MPa. New lightweight composite cylinders have been developed which are able to withstand a pressure up to 80 MPa and so the hydrogen can reach a volumetric density of 36 kg·m^{-3}, approximately half as in its liquid form at normal boiling point. The gravimetric hydrogen density decreases with increasing pressure due to the increasing thickness of the walls of the pressure cylinder. The wall thickness of a cylinder capped with two hemispheres is given by the following equation:

$$\frac{d_w}{d_o} = \frac{\Delta p}{2\sigma_v + \Delta p} \tag{3}$$

where d_w is the wall thickness, d_o the outer diameter of the cylinder, Δp the overpressure and σ_V the tensile strength of the material. The tensile strength of materials varies from 50 MPa for aluminium to more than 1,100 MPa for high quality steel. Future developments of new composite materials have a potential to increase the tensile strength above that of steel with a materials density which is less than half of the density of steel. Figure 2 shows the volumetric density of hydrogen inside the cylinder and the ratio of the wall thickness to the outer diameter of the pressure cylinder for stainless steel with a tensile strength of 460 MPa. The volumetric density of hydrogen increases with pressure and reaches a maximum above 1,000 bar, depending on the tensile strength of the

Table 1 The six basic hydrogen storage methods and phenomena. The gravimetric density ρ_m, the volumetric density ρ_v, the working temperature T and pressure p are listed. RT stands for room temperature (25°C)

Storage method	ρ_m (mass%)	ρ_V (kg H_2 m^{-3})	T (°C)	p (bar)	Phenomena and remarks
High-pressure gas cylinders	13	<40	RT	800	Compressed gas (molecular H_2) in lightweight composite cylinder (tensile strength of the material is 2000 MPa)
Liquid hydrogen in cryogenic tanks	Size dependent	70.8	−252	1	Liquid hydrogen (molecular H_2), continuous loss of a few % per day of hydrogen at RT
Adsorbed hydrogen	≈2	20	−80	100	Physisorption (molecular H_2) on materials, e.g. carbon with a very large specific surface area, fully reversible
Absorbed on interstitial sites in a host metal	≈2	150	RT	1	Hydrogen (atomic H) intercalation in host metals, metallic hydrides working at RT are fully reversible
Complex compounds	<18	150	>100	1	Complex compounds ($[AlH_4]^-$ or $[BH_4]^-$), desorption at elevated temperature, adsorption at high pressures
Metals and complexes together with water	<40	>150	RT	1	Chemical oxidation of metals with water and liberation of hydrogen, not directly reversible?

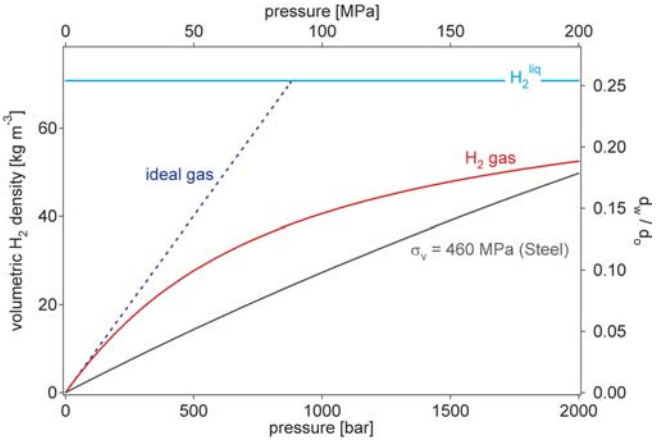

Fig. 2 Volumetric density of compressed hydrogen gas as a function of gas pressure including the ideal gas and liquid hydrogen. The ratio of the wall thickness to the outer diameter of the pressure cylinder is shown on the *right hand side* for steel with a tensile strength of 460 MPa

material. However, the gravimetric density decreases with increasing pressure and the maximum gravimetric density is found for zero overpressure! Therefore, the increase in volumetric storage density is sacrificed with the reduction of the gravimetric density in pressurized gas systems.

The safety of pressurized cylinders is an issue of concern, especially in highly populated regions. Future pressure vessels are envisaged to consist of three layers: an inner polymer liner, over-wrapped with a carbon-fibre composite (which is the stress-bearing component), and an outer layer of an aramid material capable of withstanding mechanical and corrosion damage. The target that the industry has set for itself is a 70 MPa cylinder with a mass of 110 kg, resulting in a gravimetric storage density of 6 mass% and a volumetric storage density of 30 kg·m^{-3}.

Hydrogen can be compressed using standard piston-type mechanical compressors. Slight modifications of the seals are sometimes necessary in order to compensate for the higher diffusivity of hydrogen. The theoretical work necessary for the isothermal compression of hydrogen is given by the following equation:

$$\Delta G = RT \cdot \ln\left(\frac{p}{p_0}\right) \quad (4)$$

where R stands for the gas constant (R=8.314 J·mol^{-1}·K^{-1}), T for the absolute temperature and p and p_0 for the end pressure and the starting pressure, respectively. The error of the work calculated with Eq. 3 in the pressure range of 0.1–100 MPa is less than 6%. The isothermal compression of hydrogen from 0.1 MPa to 80 MPa therefore consumes 2.21 kWh/kg. In a real process, the work consumption for compression is significantly higher because the compression is not isothermal. Metal hydrides can be used to compress hydrogen from a heat source only. Compression ratios of greater than 20:1 are possible with a final pressures of more than 100 MPa (Huston 1984).

The relatively low hydrogen density, together with the very high gas pressures in the systems, are important drawbacks of the technically simple and, on the laboratory scale, well-established high-pressure storage method.

Liquid hydrogen

Liquid hydrogen is stored in cryogenic tanks at 21.2 K at ambient pressure. Due to the low critical temperature of hydrogen (33 K), liquid hydrogen can only be stored in open systems, because there is no liquid phase existing above the critical temperature. The pressure in a closed storage system at room temperature could increase to about 10^4 bar. The volumetric density of liquid hydrogen is 70.8 kg·m^{-3} and slightly higher than that of solid hydrogen (70.6 kg·m^{-3}). The challenges of liquid hydrogen storage are the energy-efficient liquefaction process and the thermal insulation of the cryogenic storage vessel in order to reduce the boil-off of hydrogen.

The hydrogen molecule is composed of two protons and two electrons. The combination of the two electron spins only leads to a binding state if the electron spins are antiparallel. The wave function of the molecule has to be antisymmetric in view of the exchange of the space coordinates of two fermions (spin=1/2). Therefore, two groups of hydrogen molecules exist according to the total nuclear spin (I=0, antiparallel nuclear spin and I=1, parallel nuclear spin). The first group with I=0 is called para-hydrogen and the second group with I=1 is called ortho-hydrogen. Normal hydrogen at room temperature contains 25% of the para- form and 75% of the ortho-form. The ortho- form cannot be prepared in the pure state. Since the two forms differ in energy, the physical properties also differ. The melting and boiling points of parahydrogen are about 0.1 K lower than those of normal hydrogen. At zero Kelvin, all the molecules must be in a rotational ground state i.e. in the para- form.

When hydrogen is cooled from room temperature (RT) to the normal boiling point (nbp=21.2 K) the ortho-hydrogen converts from an equilibrium concentration of 75% at RT to 50% at 77 K and 0.2% at nbp. The self-conversion rate is an activated process and very slow; the half-life time of the conversion is greater than one year at 77 K. The conversion reaction from ortho- to para-hydrogen is exothermic and the heat of conversion is also temperature dependent. At 300 K the heat of conversion is 270 kJ·kg^{-1} and increases as the temperature decreases, where it reaches 519 kJ·kg^{-1} at 77 K. At temperatures lower than 77 K the enthalpy of conversion is 523 kJ·kg^{-1} and almost constant. The enthalpy of conversion is greater than the latent heat of vaporization (H_V=451.9 kJ·kg^{-1}) of normal and para-hydrogen at the nbp. If the unconverted normal hydrogen is placed in a storage vessel, the enthalpy of conversion will be released in the vessel, which leads to the evaporation of the liquid hydrogen. The transformation from ortho- to para-hydrogen can be

catalysed by a number of surface-active and paramagnetic species, e.g. normal hydrogen can be adsorbed on charcoal cooled with liquid hydrogen and desorbed in the equilibrium mixture. The conversion may take only a few minutes if a highly active form of charcoal is used. Other suitable ortho-para catalysts are metals such as tungsten, nickel, or any paramagnetic oxides like chromium or gadolinium oxides. The nuclear spin is reversed without breaking the H-H bond.

The simplest liquefaction cycle is the Joule–Thompson cycle (Linde cycle). The gas is first compressed, and then cooled in a heat exchanger, before it passes through a throttle valve where it undergoes an isenthalpic Joule–Thomson expansion, producing some liquid. The cooled gas is separated from the liquid and returned to the compressor via the heat exchanger (Flynn 1992). The Joule–Thompson cycle works for gases, such as nitrogen, with a inversion temperature above room temperature. Hydrogen, however, warms upon expansion at room temperature. In order for hydrogen to cool upon expansion, its temperature must be below its inversion temperature of 202 K. Therefore, hydrogen is usually pre-cooled using liquid nitrogen (78 K) before the first expansion step occurs. The free enthalpy change between gaseous hydrogen at 300 K and liquid hydrogen at 20 K is 11,640 $kJ \cdot kg^{-1}$ (Chen and Anghale 2003). The necessary theoretical energy (work) to liquefy hydrogen from RT is W_{th}=3.23 $kWh \cdot kg^{-1}$, the technical work is about 15.2 $kWh \cdot kg^{-1}$ (von Ardenne et al. 1990), almost half of the lower heating value of hydrogen combustion.

The boil-off rate of hydrogen from a liquid hydrogen storage vessel due to heat leaks is a function of the size, shape and thermal insulation of the vessel. Theoretically the best shape is a sphere, since it has the least surface to volume ratio and because stress and strain are distributed uniformly. However, large-sized spherical containers are expensive because of their manufacturing difficulty. Since boil-off losses due to heat leaks are proportional to the surface to volume ratio, the evaporation rate diminishes drastically as the storage tank size increases. For double-walled vacuum-insulated spherical Dewar vessels, boil-off losses are typically 0.4% per day for tanks which have a storage volume of 50 m^3, 0.2% for 100 m^3 tanks, and 0.06% for 20,000 m^3 tanks.

The relatively large amount of energy needed for the liquefaction and the continuous boil-off of hydrogen limit the possible applications for liquid hydrogen storage systems to utilizations where the cost of hydrogen is not an important issue and the hydrogen is consumed in a relatively short time, e.g. air and space applications.

Physisorption of hydrogen

The adsorption of a gas on a surface is a consequence of the field force at the surface of the solid, called the adsorbent, which attracts the molecules of the gas or vapour, called adsorbate. The origin of the physisorption of gas molecules on the surface of a solid are resonant fluctuations of the charge distributions and are therefore called dispersive interactions or Van der Waals interactions. In the physisorption process, a gas molecule interacts with several atoms at the surface of the solid. The interaction is composed of two terms: an attractive term which diminishes with the distance between the molecule and the surface to the power of −6 and a repulsive term which diminishes with the distance to the power of −12. Therefore, the potential energy of the molecule shows a minimum at a distance of approximately one molecular radius of the adsorbate. The energy minimum is of the order of 0.01–0.1 eV (1–10 $kJ \cdot mol^{-1}$ H) (London 1930a, 1930b). Due to the weak interaction, a significant physisorption is only observed at low temperatures (<273 K). Once a monolayer of adsorbate molecules is formed, the gaseous molecules interact with a surface of the liquid or solid adsorbate. Therefore, the binding energy of the second layer of adsorbate molecules is similar to the latent heat of sublimation or vaporization of the adsorbate. Consequently, the adsorption of the adsorbate at a temperature equal to or greater than the boiling point at a given pressure leads to the adsorption of one single monolayer (Brunauer at al. 1938). In order to estimate the quantity of adsorbate in the monolayer, the density of the liquid adsorbate and the volume of the molecule must be used. If the liquid is assumed to consist of a closed packed FCC structure, the minimum surface area S_{ml} for one mole of adsorbate in a monolayer on a substrate can be calculated from the density of the liquid ρ_{liq} and the molecular mass of the adsorbate M_{ads}.

$$S_{ml} = \frac{\sqrt{3}}{2}\left(\sqrt{2N_A}\cdot\frac{M_{ads}}{\rho_{liq}}\right)^{\frac{2}{3}} \quad (5)$$

N_A stands for the Avogadro constant (N_A= 6.022×10^{23} mol^{-1}). The monolayer surface area for hydrogen is $S_{ml}(H_2)$=85,917 $m^2 \cdot mol^{-1}$. The amount of adsorbate M_{ads} on a substrate material with a specific surface area S_{spec} is then given by $M_{ads}=M_{ads} \cdot S_{spec}/S_{ml}$. In the case of carbon as the substrate and hydrogen as the adsorbate, the maximum specific surface area of carbon is S_{spec}=1,315 $m^2 \cdot g^{-1}$ (single-sided graphene sheet) and the maximum amount of adsorbed hydrogen is M_{ads}=3.0 mass%. From this theoretical approximation we may conclude that the amount of adsorbed hydrogen is proportional to the specific surface area of the adsorbent with $M_{ads}/S_{spec}=2.27\times10^{-3}$ mass%$\cdot m^{-2}$ g and can only be observed at very low temperatures.

Much work on reversible hydrogen sorption of carbon nanostructures was stimulated by findings published in an article by Dillon et al. (1997). This paper describes the results of a brief hydrogen desorption experiment. The authors estimated the hydrogen storage capacity of carbon nanotubes at that time to be 5–10 mass%. The investigation was carried out on a carbon sample containing an estimated (TEM micrographs) amount of 0.1–0.2 mass% of single-wall carbon nanotubes (SWNT). The amount of hydrogen desorbed in the high-temperature peak, which is

roughly 5–10 times smaller than the low temperature physisorption peak, was 0.01 mass%. The authors concluded: "Thus the gravimetric storage density per SWNT ranges from 5 to 10 mass%". Three years later in a report to the DOE (Dillon et al. 2000) this peak has moved significantly by 300 K up to 600 K. Apparently the reported results are inconsistent. Hirscher et al. (2001) clarified the situation and showed that the desorption of hydrogen originates from Ti alloy particles in the sample, introduced during the ultrasonic treatment, rather than from the carbon nanotubes.

The main difference between carbon nanotubes and high surface area graphite is the curvature of the graphene sheets and the cavity inside the tube. In microporous solids with capillaries which have a width not exceeding a few molecular diameters, the potential fields from opposite walls will overlap so that the attractive force which acts on adsorbate molecules will be increased compared with that on a flat carbon surface (Gregg and Sing 1967). This phenomenon is the main motivation for the investigation of the hydrogen interaction with carbon nanotubes.

Most papers reporting theoretical studies on hydrogen absorption in carbon nanostructures focus on the physisorption of H_2 on carbon using the grand canonical Monte Carlo simulation. Stan and Cole (1998) used the Feynman (semiclassical) effective potential approximation to calculate the adsorption potential and the amount of hydrogen adsorbed on a zigzag nanotube (13,0) with a diameter of 1.018 nm. The adsorption potential was found to be 9 kJ mol^{-1} (0.093 eV) for hydrogen molecules inside the nanotubes at 50 K; the potential is about 25% higher as compared with the flat surface of graphite, due to the curvature of the surface. Therefore an increased number of carbon atoms interact with the hydrogen molecule. The ratio of hydrogen adsorbed in the tube to that on a flat surface decreases strongly with increasing temperature and is 10,000 at 50 K and 100 at 77 K. Rzepka et al. (1998) used a grand canonical ensemble Monte Carlo program to calculate the amount of absorbed hydrogen for a slit pore and a tubular geometry. The amount of absorbed hydrogen depends on the surface area of the sample, the maximum is at 0.6 mass% (p=6 MPa, T=300 K). The calculation was experimentally verified with excellent agreement. At a temperature of 77 K the amount of absorbed hydrogen is about one order of magnitude higher compared with 300 K. Williams and Eklund (2000) performed grand canonical Monte Carlo simulation of H_2 physisorption in finite-diameter carbon SWNT ropes and found an increasing amount of adsorbed hydrogen with decreasing temperature from 1.4 mass% (p=10 MPa, T=300 K) to 9.6 mass% (p=10 MPa, T=77 K). For lower hydrogen pressure this range is shifted to considerably lower amounts of adsorbed hydrogen, i.e. 0.2 mass% (p=1 MPa, T=300 K) to 5.9 mass% (p=10 MPa, T=77 K). Lee et al. (2000, 2001) have performed density-functional and density-functional-based tight binding calculations to search for hydrogen chemisorption sites on single-wall nanotubes. The investigation of the absorption of the hydrogen inside the tubes

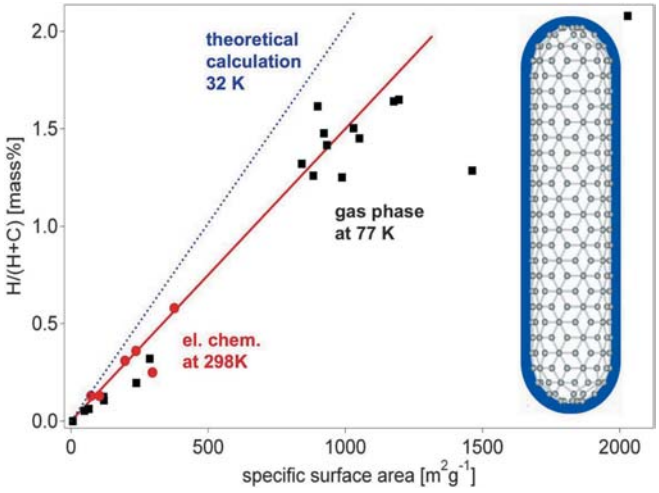

Fig. 3 Schematic drawing of reversible amount of hydrogen (electrochemical measurement at 298 K) versus the BET surface area (*round markers*) of a few carbon nanotube samples including two measurements on high-surface-area graphite (HSAG) samples together with the *fitted line*. Hydrogen gas adsorption measurements at 77 K from Nijkamp et al. (2001) (*square markers*) are included. The *dotted line* represents the calculated amount of hydrogen in a monolayer at the surface of the substrate

(Lee and Lee 2000) has shown that it is energetically more favourable for the hydrogen atoms to recombine and form molecules, which are then physisorbed inside the nanotube. Ma et al. (2001) performed a molecular dynamics simulation for H implantation. The hydrogen atoms (20 eV) were implanted through the side walls of a single-wall carbon nanotube (5,5) consisting of 150 atoms and having a diameter of 0.683 nm. They found that the hydrogen atoms recombined into molecules inside the tube and arranged themselves into a concentric tube. The hydrogen pressure inside the SWNT increases as the number of injected atoms increases and reaches 35 GPa for 90 atoms (5 mass%). This simulation does not exhibit a condensation of hydrogen inside the nanotube. The critical temperature of hydrogen (H_2) is 33.25 K (Leung et al. 1976). Therefore, at temperatures above 33.25 K and at all pressures, hydrogen does not exist as a liquid phase; hydrogen is either a gas or a solid. The density of liquid and solid hydrogen at the melting point (T_m=14.1 K) is 70.8 kg m^{-3} and 70.6 kg m^{-3}, respectively. The measurement of the latent heat of condensation of nitrogen on carbon black (Beebe et al. 1947) showed that the heat for the adsorption of one monolayer is between 11 and 12 kJ mol^{-1} (0.11–0.12 eV) and drops for subsequent layers to the latent heat of condensation for nitrogen which is 5.56 kJ mol^{-1} (0.058 eV). If we assume that hydrogen behaves in a similar manner to nitrogen, then hydrogen would only form one monolayer of liquid at the surface of carbon at temperatures above boiling point. Geometrical considerations of the nanotubes lead to the specific surface area and, therefore, to the maximum amount of condensed hydrogen in a surface monolayer. Figure 3 shows the maximum amount of hydrogen in mass% for the physi-

sorption of hydrogen on carbon nanotubes (Züttel et al. 2002). The maximum amount of adsorbed hydrogen is 2.0 mass% for single-wall carbon nanotubes (SWNT) with a specific surface area of 1,315 $m^2\ g^{-1}$ at a temperature of 77 K.

Experiments on hydrogen absorption in carbon nanostructures were carried out using different methods under various conditions and on plenty of small and often not very well characterized samples. Hydrogen gas adsorption isotherms (T=80 K) were performed by Ye et al. (1999) on purified SWNT samples. The BET surface area (total surface area based on the multipoint Brunauer, Emmett and Teller method) of the SWNT sample was found to be 285 $m^2\ g^{-1}$ and remained unchanged during hydrogen absorption and desorption. The hydrogen adsorption obtained at a temperature of 80 K and a pressure of 0.32 MPa was H/C=0.04 for the SWNT sample and was H/C=0.28 for the high-surface-area saran-carbon (1,600 $m^2\ g^{-1}$). At high hydrogen pressures (7 MPa) at a temperature of 80 K, the hydrogen to carbon ratio for the SWNT sample reached H/C=1 (7.7 mass%) in the initial absorption. In the following absorption cycles, the absorption isotherm shifted considerably to higher pressure. The hydrogen to carbon ratio of H/C=0.8 was reached at 12 MPa. Liu et al. (1999) applied high pressure (12 MPa) hydrogen gas at room temperature (298 K) to SWNT and followed the pressure change with time. The samples equilibrated after approximately 300 min and reached a maximum absorption of 4.2 mass% (H/C=0.5). About 20% of the absorbed hydrogen remained in the sample after desorption at room temperature. Fan et al. (1999) investigated the hydrogen absorption of vapour-grown carbon nanofibres with a diameter of 5 nm to 300 nm. The fibres absorbed hydrogen up to 12.38 mass% when a hydrogen pressure of 12 MPa was applied. The absorption equilibrated after 200–300 min. Chen et al. (1999) reported that a high hydrogen uptake of 14 mass% to 20 mass% can be achieved for K- and Li-doped MWNT, respectively, at a pressure of 0.1 MPa. The K-doped MWNT absorbed hydrogen at room temperature, but are chemically unstable, whereas the Li-doped MWNT are chemically stable, but require elevated temperatures (473–673 K) for maximum absorption and desorption of hydrogen. However, the increase in the mass observed upon hydrogen absorption was due to impurities such as oxygen and water and therefore were due to the oxidation of the alkali metals (Hirscher et al. 2002) rather than hydrogen uptake. A large variety of carbon samples was investigated by Ströbel et al. (1999), using a high-pressure microbalance. The BET (N_2) surface area of the samples ranged from 100 $m^2\ g^{-1}$ up to 3,300 $m^2\ g^{-1}$. The absorbed amount of hydrogen (p=12.5 MPa, T=296 K) correlates with the surface area according to the equation x(mass%)=0.0005S($m^2\ g^{-1}$) except for the nanofibre samples. The latter exhibited a rather low surface area of approximately 100 $m^2\ g^{-1}$; however, the increase in mass upon hydrogen absorption corresponds to about 1.2 mass%. The measured adsorption isotherms approximately follow the Langmuir adsorption model. Some isotherms intercept the mass axis (p=0) at x=0; others intercept at a finite mass between 0.2 and 0.4 mass%. Nijkamp et al. (2001) characterized a large number of carbonaceous sorbents using N_2 physisorption at 77 K and up to a pressure of 1 bar. The sorbents were chosen to represent a large variation in surface area and (micropore) volumes. Both non-porous materials, such as aerosil and graphites, and microporous sorbents, such as activated carbons and zeolites, were selected. The H_2 adsorption measurements were performed at 77 K in the pressure range 0–1 bar. From adsorption–desorption experiments it is evident that reversible physisorption takes place exclusively with all samples. The amount of adsorbed hydrogen correlates with the specific surface area of the sample (Fig. 3). A few papers on electrochemical measurements at room temperature of hydrogen uptake and release have been published (Nützenadel et al. 1999a, 1999b; Züttel et al 2001; Lee et al. 2000). The electrochemical hydrogen absorption is reversible. The maximum discharge capacity measured at 298 K is 2 mass% with a very small discharge current (discharge process for 1,000 h). The few round markers with the fitted line in Fig. 3 are electrochemical results. It is remarkable that the measurements of the hydrogen uptake in the gas phase at 77 K exhibit the same quantities as the electrochemical measurements at room temperature 298 K. In the electrochemical charging process, hydrogen atoms are left back at the surface of the electrode when the electron transfer from the conductor to the water molecules takes place. The hydrogen atoms recombine to form hydrogen molecules. This process goes on until the surface is completely covered with a monolayer of physisorbed H_2 molecules. Additional hydrogen does not interact with the attractive Van der Waals forces of the surface. The hydrogen molecules become very mobile and form gas bubbles, which are released from the electrode surface. The formation of a stable monolayer of hydrogen at the electrode surface at room temperature is only possible if either the hydrogen atoms or the hydrogen molecules are immobile, i.e. their surface diffusion has to be kinetically hindered by a large energy barrier probably due to the adsorbed electrolyte (H_2O) molecules in the second layer. Another possible reaction path was first reported (Lee et al. 2000) as a result of density-functional calculation. The result of this calculation is that hydrogen atoms tend to chemisorb at the exterior surface of a nanotube. The atoms can then flip in and recombine to hydrogen molecules finally at high coverage forming a concentric cylinder in the cavity of the nanotube. If the binding energy of the chemisorbed hydrogen is relatively low compared to the energy in hydrocarbons, then the absorbed amount of hydrogen is proportional to the surface area of the carbon sample and could also desorb at rather positive electrochemical potential.

In conclusion: the reversible hydrogen sorption process is based on the physisorption. The amount of adsorbed hydrogen is proportional to the BET surface area of the nanostructured carbon sample at low temperature (77 K). The amount of adsorbed hydrogen from the gas phase at 77 K and electrochemically at room temperature

is 1.5×10^{-3} mass%·m^{-2} g. Together with the maximum specific surface area of carbon (1,315 m^2 g^{-1}) the maximum absorption capacity for hydrogen on carbon nanostructures is 2 mass%. The experimental results are in good agreement with the theoretical estimations if we take into account that the measurements were carried out at a temperature of 77 K, which is still far above the critical temperature of hydrogen of 32 K, and therefore the monolayer of hydrogen is not complete at 77 K. No evidence of an influence of the geometric structure of the nanostructured carbon on the amount of absorbed hydrogen was found. It is quite obvious that the curvature of nanotubes may only influence the adsorption energy but not the amount of adsorbed hydrogen. Furthermore, all attempts to open the nanotubes and to absorb hydrogen inside the tubes did not show an increased absorption of hydrogen molecules. Theoretical studies beyond the well-known physisorption lead to a large set of various maximum hydrogen absorption capacities. Most of the results were found under special conditions, e.g. at 0 K or high-energy hydrogen atom implantation. No evidence was found for a higher density of hydrogen in and on carbon nanostructures compared to liquid hydrogen at ambient conditions. The quantity of physisorbed hydrogen at room temperature up to a pressure of 35 MPa is less than 0.1 mass% for all types of nanostructured carbon e.g. fibres, nanotubes, high-surface-area carbon (Tibbetts et al. 2001; Ritschel et al. 2002).

Beside the carbon nanostructures, other nanoporous materials have been investigated for hydrogen absorption. The hydrogen absorption of zeolites of different pore architecture and composition, e.g. A, X, Y, was analysed in the temperature range 293–573 K and pressure range 2.5–10 MPa (Weitkamp et al. 1995). Hydrogen was absorbed at the desired temperature and pressure. The sample was then cooled to room temperature and evacuated. Subsequently the hydrogen release upon heating of the sample to the absorption temperature was detected. The absorbed amount of hydrogen increased with increasing temperature and increasing absorption pressure. The maximum amount of desorbed hydrogen was found to be 0.08 mass% for a sample loaded at a temperature of 573 K and a pressure of 10 MPa. The adsorption behaviour indicates that the absorption is due to a chemical reaction rather than physisorption. At liquid nitrogen temperature (77 K) the zeolites physisorb hydrogen proportional to the specific surface area of the material. A maximum of 1.8 mass% of adsorbed hydrogen was found for a zeolite (NaY) with a specific surface area of 725 $m^2\cdot g^{-1}$ (Langmi et al. 2003). The low-temperature physisorption (type I isotherm) of hydrogen in zeolites is in good agreement with the adsorption model mentioned above for nanostructured carbon. The desorption isotherm followed the same path as the adsorption, which indicates that no pore condensation occurred. Recently a microporous metal-organic framework of the composition Zn_4O(1,4-benzenedicarboxylate)$_3$ was proposed as hydrogen storage material (Rosi et al. 2003). The material absorbs hydrogen at a temperature of 298 K proportional to the applied pressure. The slope of the linear relationship between the gravimetric hydrogen density and the hydrogen pressure was found to be 0.05 mass%·bar^{-1}. No saturation of the hydrogen absorption was found, which is very unlikely for any kind of a hydrogen absorption process. At 77 K the amount of adsorbed hydrogen was detected to be 3.7 mass% already at very low hydrogen pressure and a slight, almost linear, increase with increasing pressure. This behaviour is not a type I isotherm as the authors claimed and the results should be treated with caution.

The big advantages of the physisorption for hydrogen storage are the low operating pressure, the relatively low cost of the materials involved, and the simple design of the storage system. The rather small amount of adsorbed hydrogen on carbon, together with the low temperatures necessary, are significant drawbacks of hydrogen storage based on physisorption.

Metalhydrides

Metals, intermetallic compounds and alloys generally react with hydrogen and form mainly solid metal-hydrogen compounds. Hydrides exist as ionic, polymeric covalent, volatile covalent and metallic hydrides. The demarcation between the various types of hydrides is not sharp; they merge into each other according to the electronegativities of the elements concerned. This section focuses on metallic hydrides, i.e. metals and intermetallic compounds which form together with hydrogen metallic hydrides. Hydrogen reacts at elevated temperature with many transition metals and their alloys to form hydrides. The electropositive elements are the most reactive, i.e. scandium, yttrium, the lanthanides, the actinides, and the members of the titanium and vanadium groups. The binary hydrides of the transition metals are predominantly metallic in character and are usually referred to as metallic hydrides. They are good conductors of electricity, possess a metallic or graphite-like appearance, and can often be wetted by mercury. Many of these compounds (MH_n) show large deviations from ideal stoichiometry (n=1, 2, 3) and can exist as multi-phase systems. The lattice structure is that of a typical metal with atoms of hydrogen on the interstitial sites; for this reason they are also called interstitial hydrides. This type of structure has the limiting compositions MH, MH_2 and MH_3; the hydrogen atoms fit into octahedral or tetrahedral holes in the metal lattice, or a combination of the two types. The hydrogen carries a partial negative charge, depending on the metal; an exception is, for example, $PdH_{0.7}$ (Pearson 1985). Only a small number of the transition metals are without known stable hydrides. A considerable “hydride gap” exists in the periodic table, beginning at group 6 (Cr) up to group 11 (Cu), in which the only hydrides are palladium hydride ($PdH_{0.7}$), the very unstable nickel hydride ($NiH_{<1}$), and the poorly defined hydrides of chromium (CrH, CrH_2) and copper (CuH). In palladium hydride, the hydrogen has high mobility and

Table 2 The most important families of hydride-forming intermetallic compounds including the prototype and the structure. A is an element with a high affinity to hydrogen, and B is an element with a low affinity to hydrogen

Intermetallic compound	Prototype	Hydrides	Structure
AB_5	$LaNi_5$	$LaNiH_6$	Haucke phases, hexagonal
AB_2	ZrV_2, $ZrMn_2$, $TiMn_2$	$ZrV_2H_{5.5}$	Laves phase, hexagonal or cubic
AB_3	$CeNi_3$, YFe_3	$CeNi_3H_4$	Hexagonal, $PuNi_3$-type
A_2B_7	Y_2Ni_7, Th_2Fe_7	$Y_2Ni_7H_3$	Hexagonal, Ce_2Ni_7-type
A_6B_{23}	Y_6Fe_{23}	$Ho_6Fe_{23}H_{12}$	Cubic, Th_6Mn_{23}-type
AB	TiFe, ZrNi	$TiFeH_2$	Cubic, CsCl- or CrB-type
A_2B	Mg_2Ni, Ti_2Ni	Mg_2NiH_4	Cubic, $MoSi_2$- or Ti_2Ni-type

probably a very low charge density. In the finely divided state, platinum and ruthenium are able to adsorb considerable quantities of hydrogen, which thereby becomes activated. These two elements, together with palladium and nickel, are extremely good hydrogenation catalysts, although they do not form hydrides (Müller et al. 1968). Especially interesting are the metallic hydrides of intermetallic compounds; in the simplest case the ternary system AB_xH_n, because the variation of the elements allows tailoring of the properties of the hydrides (see Table 2). The A element is usually a rare earth or an alkaline earth metal and tends to form a stable hydride. The B element is often a transition metal and forms only unstable hydrides. Some well defined ratios of B to A in the intermetallic compound x=0.5, 1, 2, 5 have been found to form hydrides with a hydrogen to metal ratio of up to 2.

The reaction of hydrogen gas with a metal is called the absorption process and can be described in terms of a simplified one-dimensional potential energy curve (one-dimensional Lennard-Jones potential) (Lennard-Jones 1932). Far from the metal surface the potential of a hydrogen molecule and of 2 hydrogen atoms are separated by the dissociation energy (H_2 –>2H, E_D=435.99 kJ·mol^{-1}). The first attractive interaction of the hydrogen molecule approaching the metal surface is the Van der Waals force leading to the physisorbed state (E_{Phys}≈10 kJ·mol^{-1} H) approximately one hydrogen molecule radius (≈0.2 nm) from the metal surface. Closer to the surface the hydrogen has to overcome an activation barrier for dissociation and formation of the hydrogen metal bond. The height of the activation barrier depends on the surface elements involved. Hydrogen atoms sharing their electron with the metal atoms at the surface are then in the chemisorbed state (E_{Chem}≈50 kJ·mol^{-1} H_2). The chemisorbed hydrogen atoms may have a high surface mobility, interact with each other and form surface phases at sufficiently high coverage. In the next step the chemisorbed hydrogen atom can jump in the subsurface layer and finally diffuse on the interstitial sites through the host metal lattice (Schlapbach 1992). The hydrogen atoms contribute with their electron to the band structure of the metal. The hydrogen is present at a small hydrogen to metal ratio (H/M<0.1) exothermically dissolved (solid-solution, α-phase) in the metal. The metal lattice expands proportionally to the hydrogen concentration by approximately 2–3Å^3 per hydrogen atom (Fukai 1989). At greater hydrogen concentrations in the host metal (H/M>0.1) a strong H–H interaction due to the lattice expansion becomes important and the hydride phase

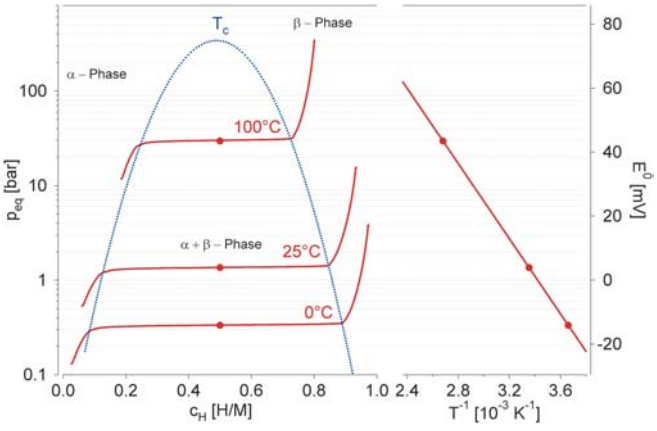

Fig. 4 Pressure composition isotherms for the hydrogen absorption in a typical intermetallic compound is shown on the *left hand side*: comprising the solid solution (α-phase), the hydride phase (β-phase) and the region where the two phases coexist. The coexistence region is characterized by the flat plateau and ends at the critical temperature T_c. The construction of the Van't Hoff plot is shown on the *right hand side*. The *slope of the line* is equal to the enthalpy of formation divided by the gas constant and the interception is equal to the entropy of formation divided by the gas constant

(β-phase) nucleates and grows. The hydrogen concentration in the hydride phase is often found to be H/M=1. The volume expansion between the coexisting α- and the β-phase corresponds in many cases to 10–20% of the metal lattice. Therefore, at the phase boundary a large amount of stress is built up and often leads to a decrepitation of brittle host metals such as intermetallic compounds. The final hydride is a powder with a typical particle size of 10–100 μm.

The thermodynamic aspects of the hydride formation from gaseous hydrogen is described by means of pressure-composition isotherms (see Fig. 4). While the solid solution and hydride phase coexists, the isotherms show a flat plateau, the length of which determines the amount of H_2 stored. In the pure β-phase, the H_2 pressure rises steeply with the concentration. The two-phase region ends in a critical point T_C, above which the transition from α- to β-phase is continuous. The equilibrium pressure p_{eq} as a function of temperature is related to the changes ΔH and ΔS of enthalpy and entropy, respectively, by the Van't Hoff equation:

$$\ln\left(\frac{p_{eq}}{p^0_{eq}}\right) = \frac{\Delta H}{R}\cdot\frac{1}{T} - \frac{\Delta S}{R} \qquad (6)$$

As the entropy change corresponds mostly to the change from molecular hydrogen gas to dissolved solid hydrogen, it amounts approximately to the standard entropy of hydrogen (S^0=130 J·K^{-1}mol^{-1}) and is therefore, $\Delta S_f \approx ^{-1}30$ J·K^{-1}mol^{-1}H$_2$ for all metal–hydrogen systems. The enthalpy term characterizes the stability of the metal hydrogen bond. To reach an equilibrium pressure of 1 bar at 300 K, ΔH should amount to 39.2 kJ mol^{-1}H$_2$. The entropy of formation term of metal hydrides leads to a significant heat evolution $\Delta Q = T \cdot \Delta S$ (exothermal reaction) during the hydrogen absorption. The same heat has to be provided to the metal hydride to desorb the hydrogen (endothermal reaction). If the hydrogen desorbs below room temperature, this heat can be delivered by the environment. However, if the desorption is carried out above room temperature, the necessary heat has to be delivered at the necessary temperature from an external source which may be the combustion of the hydrogen. For a stable hydride like MgH$_2$ the heat necessary for the desorption of hydrogen at 300°C and 1 bar is approximately 25% of the higher heating value of hydrogen.

Several empirical models allow the estimation of the stability and the concentration of hydrogen in an intermetallic hydride. The maximum amount of hydrogen in the hydride phase is given by the number of interstitial sites in the intermetallic compound for which to following two criteria apply. The distance between two hydrogen atoms on interstitial sites is at least 2.1 Å (Switendick 1979) and the radius of the largest sphere on an interstitial site touching all the neighbouring metallic atoms is at least 0.37 Å (Westlake criterion) (Westlake 1983). The theoretical maximum volumetric density of hydrogen in a metal hydride, assuming a closed packing of the hydrogen, is therefore 253 kg·m^{-3}, which is 3.6 times the density of liquid hydrogen. As a general rule, it can be stated that all elements with an electronegativity in the range 1.35–1.82 do not form stable hydrides (Rittmeyer and Wietelmann (1989). Exemptions are vanadium (1.45) and chromium (1.56), which form hydrides, and molybdenum (1.30) and technetium (1.36), where hydride formation would be expected. The adsorption enthalpy can be estimated from the local environment of the hydrogen atom on the interstitial site. According to the rule of imaginary binary hydrides, the stability of a hydrogen on an interstitial site is the weighted average of the stability of the corresponding binary hydrides of the neighbouring metallic atoms (Miedema 1973). More general is the rule of reversed stability (Miedema model): the more stable a intermetallic compound the less stable is the corresponding hydride and the other way around (Van Mal et al. 1974). This model is based on the fact that hydrogen can only participate on a bond with a neighbouring metal atom if the bonds between the metal atoms are at least partially broken. Hydrogen absorption is electronically an incorporation of electrons and protons into the electronic structure of the host lattice. The electrons have to fill empty states at the Fermi energy E_F while the protons lead to the hydrogen induced *s*-band approximately 4 eV below the E_F. The heat of formation of binary hydrides

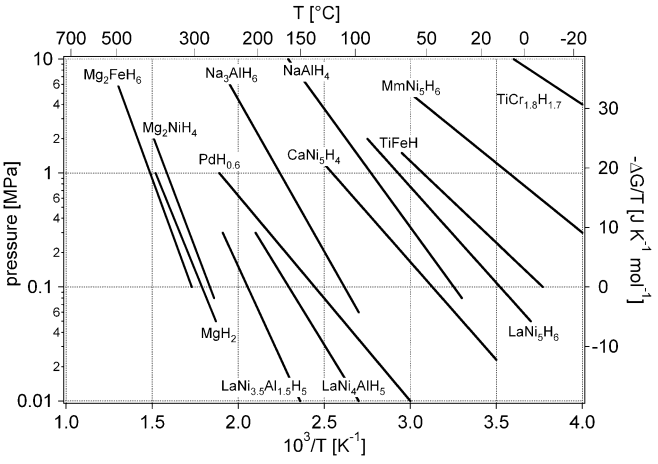

Fig. 5 Van't Hoff plots of some selected hydrides. The stabilization of the hydride of $LaNi_5$ by the partial substitution of nickel with aluminium in $LaNi_5$ is shown as well as the substitution of lanthanum with mischmetal (e.g. 51% La, 33% Ce, 12% Nd, 4% Pr)

MH_x is related linearly to the characteristic band energy parameter $\Delta E = E_F - E_s$, where E_F is the Fermi energy and E_s the centre of the host metal electronic band with a strong *s* character at the interstitial sites occupied by hydrogen. For most metals E_s can be taken as the energy which corresponds to one electron per atom on the integrated density-of-states curve (Griessen and Driessen 1983).

The semi-empirical models mentioned above allow an estimation of the stability of binary hydrides as long as the rigid band theory can be applied. However, the interaction of hydrogen with the electronic structure of the host metal in some binary hydrides, and especially in the ternary hydrides, is often more complicated. In many cases the crystal structure of the host metal, and therefore also the electronic structure, changes upon the phase transition and the theoretical calculation of the stability of the hydride becomes very complicated, if not impossible. The stability of metal hydrides is usually presented in the form of Van't Hoff plots according to Eq. 6 (see Fig. 5). The most stable binary hydrides have enthalpies of formation of $\Delta H_f = ^{-2}26$ kJ·mol^{-1}H$_2$, e.g. HoH$_2$. The least stable hydrides are $FeH_{0.5}$, $NiH_{0.5}$ and $MoH_{0.5}$, with enthalpies of formation of ΔH_f=+20 kJ·mol^{-1} H$_2$, ΔH_f= +20 kJ·mol^{-1} H$_2$, and ΔH_f=+92 kJ·mol^{-1} H$_2$, respectively (Griessen and Riesterer 1988).

Due to the phase transition upon hydrogen absorption, metal hydrides have the very useful property of absorbing large amounts of hydrogen at a constant pressure, i.e. the pressure does not increase with the amount of hydrogen absorbed as long as the phase transition takes place. The characteristics of the hydrogen absorption and desorption can be tailored by partial substitution of the constituent elements in the host lattice. Some metal hydrides absorb and desorb hydrogen at ambient temperature and close to atmospheric pressure. Several families of intermetallic compounds listed in Table 2 are of interest for hydrogen

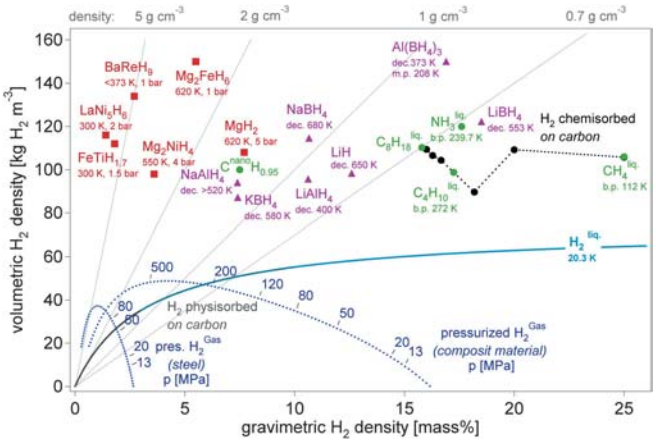

Fig. 6 Volumetric and gravimetric hydrogen density of some selected hydrides. Mg_2FeH_6 shows the highest known volumetric hydrogen density of 150 kg·m^{-3}, which is more than double that of liquid hydrogen. $BaReH_9$ has the largest H/M ratio of 4.5, i.e. 4.5 hydrogen atoms per metal atom. $LiBH_4$ exhibits the highest gravimetric hydrogen density of 18 mass%. Pressurized gas storage is shown for steel (tensile strength σ_v=460 MPa, density 6,500 kg·m^{-3}) and a hypothetical composite material (σ_v=1,500 MPa, density 3,000 kg·m^{-3})

storage. They all consist of an element with a high affinity to hydrogen, the A-element, and an element with a low affinity to hydrogen, the B-element. The latter is often at least partially nickel, since nickel is an excellent catalyst for the hydrogen dissociation.

One of the most interesting features of the metallic hydrides is the extremely high volumetric density of the hydrogen atoms present in the host lattice (see Fig. 6). The highest volumetric hydrogen density known today is 150 kg·m^{-3} found in Mg_2FeH_6 and $Al(BH_4)_3$. Both hydrides belong to the complex hydrides and will be discussed in the next section. Metallic hydrides reach a volumetric hydrogen density of 115 kg·m^{-3} e.g. $LaNi_5$. Most metallic hydrides absorb hydrogen up to a hydrogen to metal ratio of H/M=2. Greater ratios up to H/M=4.5, e.g. $BaReH_9$ (Yvon 1998), have been found; however, all hydrides with a hydrogen to metal ratio of >2 are ionic or covalent compounds and belong to the complex hydrides.

Metal hydrides are very effective for storing large amounts of hydrogen in a safe and compact way. All the reversible hydrides working around ambient temperature and atmospheric pressure consist of transition metals; therefore the gravimetric hydrogen density is limited to <3 mass%. It is still a challenge to explore the properties of the lightweight metal hydrides.

Complex hydrides

The group one, two and three light elements (e.g. Li, Mg, B, Al) build a large variety of metal–hydrogen complexes. They are especially interesting because of their light weight and the number of hydrogen atoms per metal atom, which is in many cases 2. The main difference of the complex hydrides to the above-described metallic hydrides is the transition to an ionic or covalent compound of the metals upon hydrogen absorption. The hydrogen in the complex hydrides is often located in the corners of a tetrahedron with boron or aluminium in the centre. The negative charge of the anion, $[BH_4]^-$ and $[AlH_4]^-$, is compensated by a cation, e.g. Li or Na. The hydride complexes of borane, the tetrahydroborates $M(BH_4)$, and of alane the tetrahydroaluminate $M(AlH_4)$ are interesting storage materials; however, they are known to be stable and decompose only at elevated temperatures and often above the melting point of the complex.

Bogdanović and Schwickardi (1997) presented in 1996 for the first time adsorption and desorption pressure-concentration isotherms of catalysed $NaAlH_4$ at temperatures of 180°C and 210°C. The isotherms exhibit an absence of hysteresis and a nearly horizontal pressure plateau. Furthermore, the catalysed system reversibly absorbed and desorbed hydrogen up to 4.2 mass% and the mechanism of the two-step reaction was described. A more detailed study of the $NaAlH_4$ with an improved catalyst was published by Bogdanović et al. (2000). A desorption hydrogen pressure of 2 bar at 60°C was found and the enthalpy for the dissociation reaction was determined to be 37 kJ·mol^{-1} and 47 kJ·mol^{-1} for the first dissociation step of Ti-doped $NaAlH_4$: 3 $NaAlH_4 \rightarrow Na_3AlH_6 + 2\ Al + 3\ H_2$ (3.7 wt% H) and the second $Na_3AlH_6 \rightarrow 3NaH + Al + 3/2\ H_2$ (3.0 wt% H), respectively. Therefore, the equilibrium hydrogen pressure at room temperature is approximately 1 bar. Furthermore, the reaction is reversible, a complete conversion to product was achieved at 270°C under 175 bar hydrogen pressure in 2–3 h (Dymova et al. 1974). $Mg(AlH_4)_2$ contains 9.6 mass% of hydrogen and decomposes below 200°C. The compound was recently successfully synthesized and the structure of the compound together with the solvent was analysed (Fichtner and Fuhr 2002). The direct determination of the structure of pure $Mg(AlH_4)_2$ was not possible, because no single crystals could be obtained from the substance.

The first report of a pure alkali metal tetrahydroboride appeared in 1940 from Schlesinger and Brown (1940) who synthesized the lithiumtetrahydroboride (lithiumborohydride) ($LiBH_4$) by the reaction of ethyllithium with diborane (B_2H_6). The direct reaction of the corresponding metal with diborane in etheral solvents under suitable conditions produces high yields of the tetrahydroborides (Schlesinger et al. 1953) $2\ MH + B_2H_6 \rightarrow 2\ MBH_4$ where M=Li, Na, K etc. Direct synthesis from the metal, boron and hydrogen at 550–700°C and 30–150 bar H_2 has been reported to yield the lithium salt, and it has been claimed that such a method is generally applicable to group IA and IIA metals (Görrig 1958). The reaction involving either the metal or the metal hydride, or the metal together with triethylborane in an inert hydrocarbon, has formed the basis of a patent $M + B + 2H_2 \rightarrow MBH_4$, where M=Li, Na, K etc.

The stability of metal tetrahydroborides has been discussed in relation to their percentage ionic character, and those compounds with less ionic character than diborane are expected to be highly unstable (Schrauzer 1955). Steric effects have also been suggested to be important in some compounds (Lippard and Ucko 1968). The special feature exhibited by the covalent metal hydroborides is that the hydroboride group is bonded to the metal atom by bridging hydrogen atoms similar to the bonding in diborane, which may be regarded as the simplest of the so called "electron-deficient" molecules. Such molecules possess fewer electrons than those apparently required to fill all the bonding orbitals, based on the criterion that a normal bonding orbital involving two atoms contains two electrons. The molecular orbital bonding scheme for diborane has been discussed extensively (Lipscomb 1963).

The compound with the highest gravimetric hydrogen density at room temperature known today is $LiBH_4$ (18 mass%). Therefore, this complex hydride could be the ideal hydrogen storage material for mobile applications. $LiBH_4$ desorbs three of the four hydrogen in the compound upon melting at 280°C and decomposes into LiH and boron. The desorption process can be catalysed by adding SiO_2 and significant thermal desorption was observed starting at 100°C (Züttel et al. 2003). Recently it has been shown that the hydrogen desorption reaction is reversible and the end-products lithimhydride and boron absorb hydrogen at 690°C and 200 bar to form $LiBH_4$ (Sudan et al. 2004). The scientific understanding of the mechanism of the thermal hydrogen desorption from $LiBH_4$ and the absorption remains a challenge and more research work needs to be carried out. Very little is known yet about $Al(BH_4)_3$, a complex hydride with a very high gravimetric hydrogen density of 17 mass% and the highest known volumetric hydrogen density of 150 $kg \cdot m^{-3}$. Furthermore, $Al(BH_4)_3$ has a melting point of −65°C and is liquid at room temperature. Besides the covalent hydrocarbons, this is the only liquid hydride at room temperature.

The complex hydrides represent a very interesting and challenging new hydrogen storage material. However, very little is known about the stability, the sorption kinetics and the reversibility, since most of the complex hydrides do not exist as intermetallic compounds when the hydrogen is removed.

Chemical reaction with water

Hydrogen can be generated from metals and chemical compounds reacting with water. The most common experiment – shown in many chemistry classes – where a piece of sodium floating on water produces hydrogen, demonstrates such a process. The sodium is transformed into sodium hydroxide in this reaction. The reaction is not directly reversible but the sodium hydroxide could later be removed and reduced in a solar furnace back to metallic sodium. Two sodium atoms react with two water molecules and produce one hydrogen molecule. The hydrogen molecule produces again a water molecule in the combustion, which can be recycled to generate more hydrogen gas. However, the second water molecule necessary for the oxidation of the two sodium atoms has to be added. Therefore, sodium has a gravimetric hydrogen density of 3 mass%. The same process carried out with lithium leads to a gravimetric hydrogen density of 6.3 mass%. The major challenge with this storage method is the reversibility and the control of the thermal reduction process in order to produce the metal in a solar furnace. The process has been successfully demonstrated with zinc (Steinfeld 2002). The first, endothermic step is the thermal dissociation of ZnO(s) into Zn(g) and O_2 at 2,300 K using concentrated solar energy as the source of process heat. The second, non-solar, exothermic step is the hydrolysis of Zn(l) at 700 K to form H_2 and ZnO(s); the latter separates naturally and is recycled to the first step. Hydrogen and oxygen are derived in different steps, thereby eliminating the need for high-temperature gas separation. A second-law analysis performed on the closed cyclic process indicates a maximum exergy conversion efficiency of 29% (ratio of ΔG ($H_2 + 0.5\ O_2 \rightarrow H_2O$) for the H_2 produced to the solar power input), when using a solar cavity-receiver operated at 2,300 K and subjected to a solar flux concentration ratio of 5,000. The major sources of irreversibility are associated with the re-radiation losses from the solar reactor and the quenching of Zn(g) and O_2 to avoid their recombination. An economic assessment for a large-scale chemical plant, having a solar thermal power input into the solar reactor of 90 MW and a hydrogen production output from the hydrolyser of 61 GWh/year, indicates that the cost of solar hydrogen ranges between $0.13 and $0.15/kWh (based on its low heating value and a heliostat field cost at $100–150/$m^2$) and, thus, might be competitive vis-à-vis other renewables-based routes such as electrolysis of water using solar-generated electricity. The economic feasibility of the proposed solar process is strongly dependent on the development of an effective Zn/O_2 separation technique (either by quench or by in-situ electrolytic separation) that eliminates the need for an inert gas.

Another indirect way of using hydrogen are complex hydrides dissolved in water as a fuel. Borohydrides in alkaline media are potential fuels for fuel cells due to their high energy and power density. The borohydride-fuelled cell shows an open-circuit voltage of 1.3 V, compared with 1.0 V for a hydrogen gas-fuelled one. The actual anodic reaction of borohydride on the Ni electrode is a four-electron process (and the efficiency of the system is currently less than 50% due to hydrogen evolution (Li et al. 2003; Liu et al. 2003). The system is not directly reversible; therefore, an external energy efficient process for the production of the borohydride solution has to be developed.

Visions for the future

Hydrogen is likely to be the synthetic fuel for the future because of its large heating value and the possibility of using hydrogen produced from renewable energy in a closed cycle. However, just as the fossil fuels started the industrial age, hydrogen will start an economic and technical revolution. Once the investments for the production of renewable energy have been made, human beings will be able to profit from a hydrogen-based environmentally clean energy economy. Hydrogen will be stored in various ways depending on the application, e.g. mobile or stationary. Today we know about several efficient and safe ways to store hydrogen; however, there are many other new potential materials and methods to store hydrogen. The material science challenge is to better understand the electronic behaviour of the interaction of hydrogen with other elements and especially metals. Complex compounds like $Al(BH_4)_3$ have to be investigated and new compounds from the lightweight metals and hydrogen will be discovered. Based on today best technology, a car powered with an internal combustion engine consumes 2.4 kg (3 l) of gasoline per 100 km. Energetically this corresponds to 0.8 kg of hydrogen per 100 km. In order to drive the car for 500 km before refilling the hydrogen storage system, the car needs 4 kg of hydrogen on board. The tank with 4 kg hydrogen stored in a metal hydride is about 300 kg and has a volume of approximately 60 l. Since such a storage vessel is mainly a steel compartment filled with a metallic powder, it can be used as a constructive element of the car. In this case not all of the weight of the storage system is additional weight to the car. Furthermore, energy conversion devices more efficient than the internal combustion engine, e.g. fuel cells, will be developed and will reduce the amount of hydrogen necessary on board and therefore also the weight of the storage system.

Conclusion

The hydrogen revolution following the industrial age has just started. Hydrogen production, storage and conversion has reached a technological level, although plenty of improvements and new discoveries are still possible. The storage of hydrogen is often considered as the problem causing a bottleneck in the renewable energy economy based on synthetic fuel hydrogen. Six different hydrogen storage methods have been described. Among the well-established high-pressure cylinders for laboratory applications and liquid hydrogen for air and space applications, metal hydrides and complex hydrides offer a very safe and efficient way to store hydrogen. Further scientific research and technical developments will lead to new materials with a higher volumetric and gravimetric hydrogen density. The best materials known today show a volumetric storage density of 150 $kg \cdot m^{-3}$ which can be improved by approximately 50% according to theoretical estimations.

Acknowledgements This work was supported by the Swiss federal office of energy (Bundesamt für Energie, BfE) in contract with the International Energy Agency (IEA), the Swiss Federal Office of Education and Science (BBW), the European Commission and the Science Faculty of the University of Fribourg in Switzerland.

References

Ardenne M von, Musiol G, Reball S (1990) Effekte der Physik und ihre Anwendungen. Harri Deutsch, Frankfurt-am-Main, pp 712–715

Beebe RA, Biscoe J, Smith WR, Wendell CB (1947) Heats of adsorption on carbon black. J Am Chem Soc 69:95–101

Bogdanović B, Schwickardi M (1997) Ti-doped alkali metal aluminium hydrides as potential novel reversible hydrogen storage materials. J Alloys Compounds 253/254:1–9

Bogdanović B, Brand RA, Marjanovic A, Schwickardi M, Tolle J (2000) Metal-doped sodium aluminium hydrides as potential new hydrogen storage materials. J Alloys Compounds 302:36–58

Brunauer S, Emmett PH, Teller E (1938) Adsorption of gases in multimolecular layers. J Am Chem Soc 60:309–319

Chen G, Anghaie S (2003) Based on NASA/NIST databases http://www.inspi.ufl.edu/data/h_prop_package.html

Chen P, Wu X, Lin J, Tan K L (1999) High H_2 uptake by alkali-doped carbon nanotubes under ambient pressure and moderate temperatures. Science 285:91–93

Dillon AC, Jones KM, Bekkedahl TA, Kiang CH, Bethune DS, Heben MJ (1997) Storage of hydrogen in single-walled carbon nanotubes. Nature 386:377–379

Dillon AC, Gennett T, Alleman JL, Jones KM, Parilla PA, Heben MJ (2000) Carbon nanotube materials for hydrogen storage. In: Proceedings of the 2000 DOE/NREL hydrogen program review, May 8–10 (http://www.eere.energy.gov/hydrogenandfuelcells/pdfs/28890kkk.pdf)

Dymova TN, Eliseeva NG, Bakum SI, Dergachev YM (1974) Direct synthesis of aluminium hydrides of alkaline metals in melts. Dokl Akad Nauk SSSR 215:1369–1372

Fan YY, Liao B, Liu M, Wei YL, Lu MQ, Cheng HM (1999) Hydrogen uptake in vapor-grown carbon nanofibers. Carbon 37:1649–1652

Fichtner M, Fuhr O (2002) Synthesis and structures of magnesium alanate and two solvent adducts. J Alloys Compounds 345:286–296

Flynn TM (1992) A liquification of gases. In: McGraw-Hill encyclopedia of science and technology, 7th edn, vol 10. McGraw-Hill, New York, pp 106–109

Fukai Y (1989) Site occupancy and phase stability of some metal hydrides. Z Phys Chem 164:165–174

Görrig D (1958) Verfahren zur Herstellung von Boranaten. German Patent 1,077,644, 1–4

Gregg SJ, Sing KSW (1967) Adsorption, surface area and porosity. Academic Press, London

Griessen R, Driessen A (1983) Heat of formation and band structure of binary and ternary metal hydrides. Phys Rev B 30:4372–4381

Griessen R, Riesterer T (1988) Heat of formation models. In: Schlapbach L (ed) Hydrogen in intermetallic compounds. I. Electronic, thermodynamic, and crystallographic properties. (Topics in applied physics, vol 63) Springer, Berlin Heidelberg New York, pp 219–284

GTec (2002) Product specification from GTec SA, rte de Clos-Donroux 1, 1870 Monthey, Switzerland

Hirscher M, Becher M, Haluska M, Dettlaff-Weglikowska U, Quintel A, Duesberg GS, Choi Y-M, Downes P, Hulman M, Roth S, Stepanek I, Bernier P (2001) Hydrogen storage in sonicated carbon materials. Appl Phys A 72:129–132

Hirscher M, Becher M, Haluska M, Quintel A, Skakalova V, Choi YM, Dettlaff-Weglikowska U, Roth S, Stepanek I, Bernier P,

Leonhardt A, Fink J (2002) Hydrogen storage in carbon nanostructures. J Alloys Compounds 330/332:654–658
Huston EL (1984) A liquid and solid storage of hydrogen. In: Proceedings of the 5th world hydrogen energy conference, vol 3; July 15–20, Toronto, Canada
International Energy Agency (IEA, AIE) (2002) Key world energy statistics. Economic Analysis Division
Jochem E (1991) Longterm potentials of rational energy use: the unknown possibilities of reducing greenhouse gas emissions. Energ Environ 2:31–44
Langmi HW, Walton A, Al-Mamouri MM, Johnson SR, Book D, Speight JD, Edwards PP, Gameson I, Anderson PA, Harris IR (2003) Hydrogen adsorption in zeolites A, X, Y and RHO. J Alloys Compounds 356/357:710–715
Lee SM, Lee YH (2000) Hydrogen storage in single-walled carbon nanotubes. Appl Phys Lett 76:2877–2879
Lee SM, Park KS, Choi YC, Park JS, Bok JM, Bae DJ, Nahm KS, Choi YG, Yu SC, Kim N, Frauenheim T, Lee YH (2000) Hydrogen adsorption and storage in carbon nanotubes. Synth Met 113:209–216
Lee SM, An KH, Lee YH, Seifert G, Frauenheim T (2001) Novel mechanism of hydrogen storage in carbon nanotubes. J Korean Phys Soc 38:686–691
Lennard-Jones JE (1932) Processes of adsorption and diffusion on solid surfaces. Trans Faraday Soc 28:333–359
Leung WB, March NH, Motz H (1976) Primitive phase diagram for hydrogen. Phys Lett 56A:425–426
Li ZP, Liu BH, Arai K, Suda S (2003) A fuel cell development for using borohydrides as the fuel. J Electrochem Soc 150:A868–A872
Lippard SJ, Ucko DA (1968) Transition metal borohydride complexes. II 1. The reaction of copper(I) compounds with boron hydride anions. Inorg Chem 7:1051–1056
Lipscomb WN (1963) Boron hydrides. Benjamin, New York
Liu BH, Li ZP, Suda S (2003) Anodic oxidation of alkali borohydrides catalyzed by nickel. J Electrochem Soc 150: A398–A402
Liu C, Fan YY, Liu M, Cong HT, Cheng HM, Dresselhaus MS (1999) Hydrogen storage in single-walled carbon nanotubes at room temperature. Science 286:1127–1129
London F (1930a) Zur Theorie und Systematik der Molekularkräfte. Z Phys 63:245–271
London F (1930b) Über einige Eigenschaften und Anwendungen der Molekularkräfte. Z Phys Chem 11:222–251
Ma Y, Xia Y, Zhao M, Wang R, Mei L (2001) Effective hydrogen storage in single-wall carbon nanotubes. Phys Rev B 63:115422/1–115422/6
Miedema AR (1973) The electronegativity parameter for transition metals: heat of formation and charge transfer in alloys. J Less-Common Met 32:117–136
Müller WM, Blackledge IR, Libowitz GG (eds) (1968) Metal hydrides. Academic Press, New York
Nijkamp MG, Raaymakers JEMJ, Dillen AJ van, Jong KP de (2001) Hydrogen storage using physisorption: materials demands. Appl Phys A 72:619–623
Nützenadel C, Züttel A, Schlapbach L (1999a) Electrochemical storage of hydrogen in carbon single wall nanotubes. In: Kuzmany H, Fink J, Mehring M, Roth S (eds) Electronic properties of novel materials: science and technology of molecular nanostructures. American Institute of Physics, New York, pp 462–465
Nützenadel C, Züttel A, Emmenegger C, Sudan P, Schlapbach L (1999b) Electrochemical storage of hydrogen in carbon single wall nanotubes. In: Thorpe MF (ed) Science and application of nanotubes. (Fundamental materials research series) Kluwer Academic/Plenum, pp 205–213
Pearson GR (1985) The transition-metal-hydrogen bond. Chem Rev 85:41–49
Ritschel M, Uhlemann M, Gutfleisch O, Leonhardt A, Graff A, Täschner C, Fink J (2002) Hydrogen storage in different carbon nanostructures. Appl Phys Lett 80:2985–2987
Rittmeyer P, Wietelmann U (1989) Hydrides. In: Ullmann's encyclopedia of industrial chemistry, 5th edn, vol A13. High-performance fibers to imidazole and derivatives. VCH, Weinheim, pp 199–226
Rosi NL, Eckert J, Eddaoudi M, Vodak DT, Kim J, O'Keeffe M, Yaghi OM (2003) Hydrogen storage in microporous metal-organic frameworks. Science 300:1127–1129
Rzepka M, Lamp P, Casa-Lillo MA de la (1998) Physisorption of hydrogen on microporous carbon and carbon nanotubes. J Phys Chem B102:10894–10898
Schlapbach L (1992) Surface properties and activation. In: Schlapbach L (ed) Hydrogen in intermetallic compounds II. (Topics in applied physics 67) Springer, Berlin Heidelberg New York, pp 15–95
Schlapbach L, Züttel A (2001) Hydrogen-storage materials for mobile applications. Nature 414:353–358
Schlesinger HJ, Brown HC (1940) Metallo borohydrides. III. Lithium borohydride. J Am Chem Soc 62:3429–3435
Schlesinger HJ, Brown HC, Hoekstra HR, Rapp LR (1953) Reactions of diborane with alkali metal hydrides and their addition compounds: new syntheses of borohydrides: sodium and potassium borohydrides. J Am Chem Soc 75:199–204
Schrauzer GN (1955) Über ein Peridensystem der Metallboranate. Naturwissenschaften 42:438
Shleien B, Slaback LA Jr, Birky B (1998) Handbook of health physics and radiological health, 3rd ed. Lippincott, Williams and Wilkins, Baltimore, Md., pp 6–11
Stan G, Cole MW (1998) Hydrogen adsorption in nanotubes. J Low Temp Phys 110:539–544
Steinfeld A (2002) Solar hydrogen production via a two-step water-splitting thermochemical cycle based on Zn/ZnO redox reactions. Int J Hydrogen Energ 27:611–619
Steinfeld A, Palumbo R (2001) Solar thermochemical process technology. In: Meyers RA (ed) Encyclopedia of physical science and technology, vol 15. Academic Press, pp 237–256
Ströbel R, Jörissen L, Schliermann T, Trapp V, Schütz W, Bohmhammel K, Wolf G, Garche J (1999) Hydrogen adsorption on carbon materials. J Power Sources 84:221–224
Sudan P, Züttel A, Wenger P, Mauron P (2004) $LiBH_4$ a new reversible hydrogen storage material. Nat Mat
Switendick AC (1979) Band structure calculation for metal hydride systems. Z Phys Chem NF 117:89–112
Tibbetts GG, Meisner GP, Olk CH (2001) Hydrogen storage capacity of carbon nanotubes, filaments, and vapor-grown fibers. Carbon 39:2291–2301
Urey HC, Brickwedde FG, Murphy GM (1932) A hydrogen isotope of mass 2 and its concentration. Phys Rev 40:1–15
Van Mal HH, Buschow KHJ, Miedema AR (1974) Hydrogen absorption in $LaNi_5$ and related compounds: experimental observations and their explanation. J Less-Common Met 35:65–76
Watson RT (ed) (2001) Climate change 2001: synthesis report. Published for the Intergovernmental Panel on Climate Change IPCC, Cambridge University Press, Cambridge, UK
Weast RC (ed) (1976) Handbook of chemistry and physics, 57th edn. CRC, Boca Raton
Weitkamp J, Fritz M, Ernst S (1995) Zeolites as media for hydrogen storage. Int J Hydrogen Energ 20:967–970
Westlake DJ (1983) A geometric model for the stoichiometry and interstitial site occupancy in hydrides (deuterides) of LaNi5, LaNi4Al and LaNi4Mn. J Less-Common Met 91:275–292
Williams KA, Eklund PC (2000) Monte Carlo simulations of H_2 physisorption in finite-diameter carbon nanotube ropes. Chem Phys Lett 320:352–358
Wilson SS (1981) Sadi Carnot: Technik und Theorie der Dampfmaschine. Spektrum Wiss 10:98–109
Ye Y, Ahn CC, Witham C, Fultz B, Liu J, Rinzler AG, Colbert D, Smith KA, Smalley RE (1999) Hydrogen adsorption and cohesive energy of single-walled carbon nanotubes. Appl Phys Lett 74:2307–2309

Yvon K (1998) Complex transition metal hydrides. Chimia 52:613–619

Züttel A, Sudan P, Mauron P, Emmenegger C, Kiyobayashi T, Schlapbach L (2001) Hydrogen interaction with carbon nanostructures. J Metastable Nanocrystalline Materials 11:95–102

Züttel A, Sudan P, Mauron P, Kyiobaiashi T, Emmenegger C, Schlapbach L (2002) Hydrogen storage in carbon nanostructures. Int J Hydrogen Energ 27:203–212

Züttel A, Wenger P, Rensch S, Sudan P, Mauron P, Emmenegger C (2003) LiBH4 a new hydrogen storage material. J Power Sources 5194:1–7